coupling does affect the $t_2^5(\pi^*)^1$ charge-transfer states, and hence, the MLCT transitions are also split by spin-orbit coupling contributions, although such splitting has not been distinguished in the present studies. The *cis*-$[Os(NH_3)_4(N\text{-heterocycle})_2]^{2+}$ complexes exhibit splittings of the MLCT transitions similar to those observed for ruthenium analogues due to the C_{2v} symmetry of the complexes.[63]

Conclusions

The preparative methods described make possible high-yielding syntheses of a large variety of N-heterocyclic complexes. The pentaammine(N-heterocycle)metal(III) and -metal(II) ions are of interest for a variety of reasons, including the syntheses of binuclear ions,[2,3,8-10,24,39,64] the study of π-back-bonding effects, intramolecular electron transfer,[65-67] SERS spectra for complexes absorbed onto Ag electrodes,[13-15] electron-transfer reactions, and various spectroscopic studies.[39,61,62] The results of further studies in these areas will be reported subsequently.

Acknowledgment. P.A.L. gratefully acknowledges the receipt of a CSIRO Postdoctoral Fellowship and support from the Australian Research Grants Scheme. We are also grateful to the National Science Foundation (Grant No. CHE79-08633) and National Institutes of Health (Grant No. GM13638-17) for support, to the Stanford University and Australian National University Microanalytical Services for microanalyses, and to Professor S. Isied and K. Breslauer of Rutgers University for preliminary HPLC separations.

Registry No. $[Rh(NH_3)_5(pz)](CF_3SO_3)_3$, 115244-78-5; $[Os(NH_3)_5(pzH)]Cl_4$, 115244-79-6; $[Os(NH_3)_5(pzH)](CF_3SO_3)_4$, 115244-80-9; $[Os(NH_3)_5(pz)](CF_3SO_3)_3$, 83781-35-5; $[Os(NH_3)_5(pz)]Cl_2$, 115244-81-0; $[Os(NH_3)_5(pz)]I_2$, 115244-82-1; $[Os(NH_3)_5(pz)](BF_4)_2$, 115244-83-2; $[Os(NH_3)_5(pzH)]Cl_3$, 115244-84-3; $[Ru(NH_3)_5(pz)]Cl_2$, 104626-96-2; $[Ru(NH_3)_5(pz)](BF_4)_2$, 41481-91-8; $[Co(NH_3)_5(pz)](CF_3SO_3)_3$, 73090-59-2; $[Rh(NH_3)_5(py)](CF_3SO_3)_3$, 115244-85-4; $[Rh(NH_3)_5(bpy)](CF_3SO_3)_3$, 115244-87-6; $[Co(NH_3)_5(bpy)](CF_3SO_3)_3$, 115244-88-7; $[Ru(NH_3)_5(py)]^{2+}$, 21360-09-8; $[Ru(NH_3)_5(py)]^{3+}$, 33291-25-7; $[Os(NH_3)_5(py)]^{2+}$, 70252-47-0; $[Os(NH_3)_5(py)]^{3+}$, 83781-38-8; $[Os(NH_3)_5(bpy)]Cl_3$, 115244-89-8; $[Os(NH_3)_5(4\text{-Phpy})]Cl_3$, 115244-90-1; *cis*-$[Os(NH_3)_4(4\text{-Phpy})_2]Cl_3$, 115244-91-2; $[Os(NH_3)_5(pzMe)]Cl_4$, 115244-92-3; $[Os(NH_3)_5(pzMe)](BF_4)_4$, 83781-37-7; $[Rh(NH_3)_5(OSO_2CF_3)](CF_3SO_3)_2$, 84254-57-9; $[Os(NH_3)_5(OSO_2CF_3)](CF_3SO_3)_2$, 83781-30-0; $[Os(NH_3)_5(pz)]Cl_3$, 70252-37-8; $[Ru(NH_3)_5(OSO_2CF_3)](CF_3SO_3)_2$, 84278-98-8; $[Ru(NH_3)_5(pz)](CF_3SO_3)_3$, 76584-38-8; $[Ru(NH_3)_5(pzH)](CF_3SO_3)_4$, 115244-93-4; $[Co(NH_3)_5(OSO_2CF_3)](CF_3SO_3)_3$, 115245-01-7; $[Os(NH_3)_5(bpy)]^{2+}$, 94352-56-4; $[Os(NH_3)_5(4\text{-Phpy})]^{2+}$, 115244-94-5; *cis*-$[Os(NH_3)_4(4\text{-Phpy})_2]^{2+}$, 115244-95-6; $[Os(NH_3)_5(pzMe)]^{3+}$, 115244-96-7; *cis*-$[Os(NH_3)_4(pz)_2]^{2+}$, 115244-97-8; *cis*-$[Os(NH_3)_4(pzH)(pz)]^{3+}$, 115244-98-9; $[Os(NH_3)_5(pm)]^{3+}$, 83781-39-9; $[Os(NH_3)_5(pd)]^{3+}$, 70252-41-4; $[Os(NH_3)_5(isna)]^{3+}$, 115244-99-0.

(63) Zwickel, A. M.; Creutz, C. *Inorg. Chem.* **1971**, *10*, 2395-2399.
(64) Magnuson, R. H.; Lay, P. A.; Taube, H. *J. Am. Chem. Soc.* **1983**, *105*, 2507-2509.
(65) Isied, S. S.; Taube, H. *J. Am. Chem. Soc.* **1973**, *95*, 8198-8200.
(66) Zawacky, S. K. S.; Taube, H. *J. Am. Chem. Soc.* **1981**, *103*, 3379-3387.
(67) Isied, S. S.; Vassilian, A.; Magnuson, R. H.; Schwarz, H. A. *J. Am. Chem. Soc.* **1985**, *107*, 7432-7438.

Contribution from the Department of Chemistry, The University of Michigan, Ann Arbor, Michigan 48109-1055

Preparation, Structures, and Electrochemistry of Tetranuclear Sulfido Clusters $Cp_2M_2M'_2S_{2-4}$ (M = Mo, W; M' = Fe, Co, Ni)

M. David Curtis,* P. Douglas Williams, and W. M. Butler

Received March 24, 1987

The reaction of $R_2M_2(CO)_4$ (R = C_5H_5 (Cp), C_5H_4Me (Cp'); M = Mo, W) with $Fe_2(\mu\text{-}S_2)(CO)_6$ gives high yields of the cluster $R_2Mo_2Fe_2(CO)_8(\mu_3\text{-}S)_2$, which was isolated in two isomeric forms, planar (**3**) and butterfly (**4**), where M = Mo. For M = W, the analogous W butterfly was also isolated. The reactions of $[CpMo(\mu\text{-}S)(\mu\text{-}SH)]_2$ with $Fe_2(CO)_9$, $Co_2(CO)_8$, and $Ni(CO)_4$ gave the clusters $Cp_2Mo_2Fe_2(CO)_6(\mu_3\text{-}S)_4$ (**7**), $Cp_2Mo_2Co_2(CO)_4(\mu_3\text{-}S)_2(\mu_4\text{-}S)$ (**6**), and $Cp_2Mo_2Ni_2(CO)_2(\mu_3\text{-}S)_4$ (**9**). Crystallographic data are as follows. For **3b** (R = Cp'): a = 9.219 (2), b = 6.899 (2), c = 10.441 (2) Å; α = 73.34 (2), β = 113.68 (2), γ = 95.98 (2)°; V = 582.5 (3) Å^3; Z = 1; space group $P\bar{1}$; ρ_{calcd} = 2.14 g/cm^3. For **6**: a = 10.404 (3), b = 11.015 (3), c = 9.962 (2) Å; α = 99.78 (2), β = 96.99 (2), γ = 66.11 (2)°; V = 1002.0 (4) Å^3; Z = 2; space group $P\bar{1}$; ρ_{calcd} = 2.24 g/cm^3. For **9**: a = 9.712 (2), b = 20.303 (4), c = 9.787 (1) Å; β = 98.30 (1)°; V = 1909.5 (6) Å^3; Z = 4; space group $P2_1/n$; ρ_{calcd} = 2.27 g/cm^3. The Mo-Mo distance in these clusters (and in related compounds) shows a marked dependence on the number of S atoms that bridge the Mo-Mo bond. Mo-Mo distance (Å)/number of μ-S atoms: 3.0-3.1/1, 2.8-2.9/2, 2.65-2.8/3, 2.6/4. These sulfido clusters show complex electrochemical behavior that has been ascribed to structural reorganizations of the clusters upon reduction.

Introduction

Synthetic approaches to metal cluster formation and/or alteration are varied and difficult to systematize.[1] However, several major themes may be identified for clusters with sulfido ligands. Condensation reactions that increase cluster nuclearity are well documented[2-4] and may involve initial coordination of unsaturated metal fragments to filled lone-pair orbitals on the sulfido ligand.[5-7] In the course of these reactions, the S ligand expands its connectivity ($\mu_2 \rightarrow \mu_3 \rightarrow \mu_4$).

A second approach, exploited effectively by Vahrenkamp,[8] is the transmetalation reaction. This reaction leaves the cluster nuclearity unchanged while exchanging one metal for another. The sulfide ligands in these reactions may act as the cluster "glue"

(1) Vahrenkamp, H. *Adv. Organomet. Chem.* **1983**, *22*, 209.
(2) (a) Adams, R. D.; Horvath, I. T.; Mathur, P. *Organometallics* **1984**, *3*, 623. (b) Adams, R. D.; Horvath, I. T.; Mathur, P.; Segmuller, B. E.; Yang, L. W. *Ibid.* **1983**, *2*, 1078. (c) Adams, R. D.; Foust, D. F.; Mathur, P. *Ibid.* **1983**, *2*, 990. (d) Adams, R. D.; Horvath, I. T.; Mathur, P. *J. Am. Chem. Soc.* **1983**, *105*, 7202. (e) Adams, R. D.; Horvath, I. T.; Yang, L. W. *Ibid.* **1983**, *105*, 1533.
(3) Richter, F.; Beurich, H.; Muller, M.; Gartner, N.; Vahrenkamp, H. *Chem. Ber.* **1983**, *116*, 3774.
(4) (a) Eremenko, I. L.; Pasynskii, A. A.; Gasanov, G. S.; Orazsakhatov, B.; Struchov, Y. T.; Shklover, V. E. *J. Organomet. Chem.* **1984**, *275*, 183. (b) Pasynskii, A. A.; Eremenko, I. L.; Orazsakhatov, B.; Gasanov, G. S.; Shklover, V. E.; Struchov, Y. T. *Ibid.* **1984**, *269*, 147. (c) Pasynskii, A. A.; Eremenko, I. L.; Orazsakhatov, B.; Gasanov, G. S.; Novotortsev, V. M.; Ellert, O. G.; Seifulina, Z. M. *Ibid.* **1984**, *270*, 53.
(5) (a) Adams, R. D.; Horvath, I. T.; Segmuller, B. E. *J. Organomet. Chem.* **1984**, *262*, 243. (b) Adams, R. D.; Mannig, D.; Segmuller, B. E. *Organometallics* **1983**, *2*, 149.
(6) (a) Winter, A.; Jibril, I.; Huttner, G. *J. Organomet. Chem.* **1983**, *247*, 259. (b) Hoefler, M.; Tebbe, K.-F.; Veit, H.; Weiler, N. E. *J. Am. Chem. Soc.* **1983**, *105*, 6338. (c) Darensbourg, D. J.; Zalewski, D. J. *Organometallics* **1984**, *3*, 1598. (d) Richter, F.; Vahrenkamp, H. *Angew. Chem., Int. Ed. Engl.* **1978**, *17*, 444.
(7) (a) Eremenko, I. L.; Pasynskii, A. A.; Orazsakhatov, B.; Ellert, O. G.; Novotortsev, V. M.; Kalinnikov, V. T.; Porai-Koshits, M. A.; Antsyshkina, A. S.; Dikareva, L. M.; Ostrikova, V. N.; Struchov, Y. T.; Gerr, R. G. *Inorg. Chim. Acta* **1983**, *73*, 225 and references therein. (b) Pasynskii, A. A.; Eremenko, I. L.; Orazsakhatov, B.; Kalinnikov, V. T.; Aleksandrov, G. G.; Struchov, Y. T. *J. Organomet. Chem.* **1981**, *216*, 211.
(8) (a) Richter, F.; Roland, E.; Vahrenkamp, H. *Chem. Ber.* **1984**, *117*, 2429. (b) Muller, M.; Vahrenkamp, H. *Ibid.* **1983**, *116*, 2748.

0020-1669/88/1327-2853$01.50/0

Table I. Spectroscopic Properties of the Clusters $M_2M'_2S_{2-4}$

compd	IR (KBr), cm^{-1}	^1H NMR, δ	visible λ, nm	visible $10^{-3}\epsilon$, M^{-1} cm^{-1}	mass spec, *m/e*
$Cp_2Mo_2Fe_2(CO)_8S_2$ (**4a**) (butterfly)	2055 m, m, 2010 s, 1980 s, 1955 m, 1790 ms	5.32 (s, 10 H) ($CDCl_3$)			
$Cp'_2Mo_2Fe_2(CO)_8S_2$ (**4b**) (butterfly)	2040 s, 2010 s, 1975 s, 1960 sh, 1940 s, 1975 ms	2.15 (s, 6 H), 5.11 (2 m, 8 H) ($CDCl_3$)	490 400	1.5 sh	ns[a]
$Cp_2Mo_2Fe_2(CO)_8S_2$ (**3a**) (planar)	2030 m, 1980 s, 1960 s, 1810 ms	5.27 (s, 10 H) ($CDCl_3$)			
$Cp'_2Mo_2Fe_2(CO)_8S_2$ (**3b**) (planar)	2010 s, 1955 s, 1930 s, 1800 m	2.06 (s, 6 H), 5.25 (m, 8 H) ($CDCl_3$)	660 540 465	0.73 2.5 sh	ns
$Cp'_2Mo_2Fe_2(CO)_6S_4$ (**7**)	2030 s, 1975 s	2.34 (s, 6 H), 6.16 (2 m, 8 H) ($CDCl_3$)	665 455	5.2 sh	590 (P^+ – 6CO), 511 (P^+ – 6CO – MeCp), 432 (P^+ – 6CO – 2MeCp)
$Cp'_2Mo_2Co_2(CO)_4S_3$ (**6**)	1988 s, 1957 s	1.77 (s, 6 H), 5.00 (2 m, 8 H) (C_6D_6)	665 540 460	1.8 sh sh	676 (P^+), 648 (P^+ – CO), 620 (P^+ – 2CO), 592 (P^+ – 3CO), 564 (P^+ – 4CO)
$Cp_2W_2Fe_2(CO)_8S_2$ (**4w**) (butterfly)	2040 ms, 2015 s, 2010 s, 1970 s, 1950 s, 1790 ms	5.47 (s, 10 H) ($CDCl_3$)			ns
$Cp'_2Mo_2Ni_2(CO)_2S_4$ (**9**)	1990 s, 1970 s	1.99 (s, 6 H), 5.37 (2 m, 8 H) ($CDCl_3$)	580 450	1.8 sh	ns
$(Cp'Mo)_2(CpNi)_2S_4$ (**10**)		2.52 (s, 6 H), 4.11 (s, 10 H), 6.46 (m, 8 H) ($CDCl_3$)	655 530 405	sh sh 19	726 (P^+), 661 (P^+ – Cp), 596 (P^+ – 2Cp), 517 (P^+ – 2Cp – MeCp), 438 (P^+ – 2Cp – 2MeCp)

[a] ns indicates the compound was not stable at the probe temperature necessary for vaporization.

that prevents complete cluster degradation during the exchange reaction.

A third theme in controlled sulfide cluster synthesis utilizes the oxidative addition of a low-valent-metal complex into the S–S bond of a coordinated disulfido ligand (S_2^{2-}) as illustrated in eq 1.[9-13]

(1)

Similar reactivities are often observed for dinuclear μ-sulfido complexes[14,15] although it is difficult to determine if the reactive species is a bis(μ-sulfido) (I) or a μ-disulfido (II) complex because these species are interconvertible by an internal redox process (eq 2).[16]

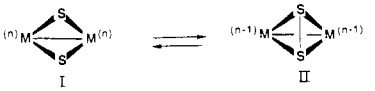

(2)

This paper reports the preparation, structures, and electrochemistry of a series of tetranuclear sulfido clusters of the general formula $Cp_2M_2M'_2L_nS_{2-4}$ (M = Mo, W; M' = Fe, Co, Ni). These clusters, comprising of early and late transition metals, are interesting as models for the active site in "sulfided" iron, cobalt, and nickel molybdate hydrotreating catalysts,[17] and as precursors for novel, sulfur-resistant CO hydrogenation and hydrodesulfurization (HDS) catalysts.[18] Some of these results have been communicated in preliminary form.[19,20]

Results and Discussion

Synthesis. (a) $Cp_2Mo_2Fe_2(CO)_8S_2$. Our initial strategy for the synthesis of Mo–sulfido clusters was guided by the known reactivities of the Mo≡Mo triple bond toward electrophilic S—S bonds[21,22] and the oxidative addition reactions of $Fe_2(S_2)(CO)_6$ (**2**) with low-valent-metal complexes.[13]

In fact, complexes **1** and **2** react to give a mixture of isomeric clusters **3** and **4** (eq 3). Clusters **3a** and **4a** were obtained in a

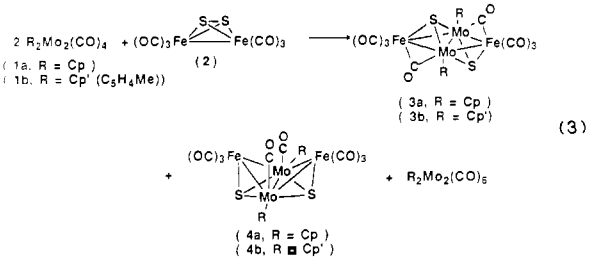

(3)

1:1.7 ratio (55% yield), and **3b** and **4b** in a 1:4 ratio (ca. 80%

(9) Some recent examples include: (a) Draganjac, M.; Simhon, E.; Chan, L. T.; Kanatzidis, M.; Baenziger, N. C.; Coucouvanis, D. *Inorg. Chem.* **1982**, *21*, 3321. (b) Goh, L. Y.; Hambley, T. N.; Robertson, G. B. *J. Chem. Soc., Chem. Commun.* **1983**, 1458. (c) Herrmann, W. A.; Rohrmann, J.; Schafer, A. *J. Organomet. Chem.* **1984**, *265*, C1. (d) Koch, S.; Chebolu, V. *Organometallics* **1983**, *2*, 350. (e) Manoli, J. M.; Bregeault, J. M.; Potvin, C.; Chottard, G. *Inorg. Chim. Acta* **1984**, *88*, 75. (f) Muller, A.; Eltzner, W.; Jostes, R.; Bogge, H.; Diemann, E.; Schimanski, J.; Lueken, H. *Angew. Chem., Int. Ed. Engl.* **1984**, *23*, 389. (g) Pan, W.-H.; Harmer, M. A.; Halbert, T. R.; Stiefel, E. I. *J. Am. Chem. Soc.* **1984**, *106*, 459.

(10) (a) Brunner, H.; Meier, W.; Wachter, J.; Guggolz, E.; Zahn, T.; Ziegler, M. L. *Organometallics* **1982**, *1*, 1107. (b) Brunner, H.; Wachter, J.; Guggolz, E.; Ziegler, M. L. *J. Am. Chem. Soc.* **1982**, *104*, 1765.

(11) (a) Bolinger, C. M.; Rauchfuss, T. B.; Rheingold, A. L. *J. Am. Chem. Soc.* **1983**, *105*, 6321. (b) Bolinger, C. M.; Rauchfuss, T. B.; Rheingold, A. L. *Organometallics* **1982**, *1*, 1551.

(12) Ginsberg, A. P.; Lindsell, W. E.; Sprinkle, C. R.; West, K. W.; Cohen, R. L. *Inorg. Chem.* **1982**, *21*, 3666.

(13) (a) Seyferth, D.; Henderson, R. S.; Gallagher, M. K. *J. Organomet. Chem.* **1980**, *193*, C75. (b) Seyferth, D.; Henderson, R. C.; Fackler, J. P.; Mazany, A. M. *Ibid.* **1981**, *213*, C21.

(14) (a) Bolinger, C. M.; Rauchfuss, T. B.; Wilson, S. R. *J. Am. Chem. Soc.* **1982**, *104*, 7313. (b) Rauchfuss, T. B.; Weatherill, T. D.; Wilson, S. R.; Zebrowski, J. P. *Ibid.* **1983**, *105*, 6508.

(15) (a) Brunner, H.; Kauermann, H.; Wachter, J. *J. Organomet. Chem.* **1984**, *265*, 189. (b) Brunner, H.; Kauermann, H.; Wachter, J. *Angew. Chem., Int. Ed. Engl.* **1983**, *22*, 549. (c) Brunner, H.; Wachter, J. *J. Organomet. Chem.* **1982**, *240*, C41.

(16) (a) Rakowski DuBois, M.; DuBois, D. L.; VanDerveer, M. C.; Haltiwanger, R. C. *Inorg. Chem.* **1981**, *20*, 3064. (b) Rakowski DuBois, M.; Haltiwanger, R. C.; Miller, D. J.; Glatzmaier, G. *J. Am. Chem. Soc.* **1979**, *101*, 5245.

(17) (a) Grange, P. *Catal. Rev.—Sci. Eng.* **1980**, *22*, 401. (b) Ratnasamy, P.; Sivasanker, S. *Ibid.* **1980**, *22*, 401. (c) Topsoe, N. Y.; Topsoe, H. *J. Catal.* **1983**, *84*, 386 and references therein.

(18) (a) Curtis, M. D.; Schwank, J.; Thompson, L.; Williams, P. D.; Baralt, O. *Prepr. Pap.—Am. Chem. Soc., Div. Fuel Chem.* **1986**, *31*, 44. (b) Curtis, M. D.; Schwank, J.; Williams, P. D.; Thompson, L. T. U.S. Patent 4 605 751, 1986. (c) Curtis, M. D.; Penner-Hahn, J. E.; Schwank, J.; Baralt, O.; McCabe, D. J.; Thompson, L.; Waldo, G. *Polyhedron*, in press.

(19) Williams, P. D.; Curtis, M. D.; Duffy, D. N.; Butler, W. M. *Organometallics* **1983**, *2*, 165.

(20) Curtis, M. D.; Williams, P. D. *Inorg. Chem.* **1983**, *22*, 2661. Note: The $LiEt_3BH:Cp_2Mo_2S_x$ ratio reported in this reference is incorrect. This ratio should be 11 mequiv of $LiEt_3BH$:g of sulfide.

(21) Curtis, M. D.; Klingler, R. J. *J. Organomet. Chem.* **1978**, *161*, 23.

(22) Curtis, M. D.; Butler, W. M. *J. Chem. Soc., Chem. Commun.* **1980**, 998.

yield), according to the stoichiometry shown in eq 3. The synthesis and characterization of **4a** and the Cr analogue, $Cp_2Cr_2Fe_2S_2(CO)_8$, has also been reported by Braunstein et al.[23] in work done concurrently with our own.

In agreement with the X-ray-determined structures (see below), the IR spectra of **3** and **4** show the presence of $Fe(CO)_3$ groups and bridging CO's (ν_{CO} = 1790–1810 cm^{-1}), and the ^1H NMR spectra show symmetry-equivalent Cp groups (spectroscopic data are collected in Table I). The ^{13}C NMR data for **4b** show peaks at δ 15.1 (Cp*Me*) and 91.7, 92.9, and 113.2 (Cp) but only two peaks for the carbonyl carbon atoms at δ 210.7 ($Fe(CO)_3$) and 238.3 (μ-CO). In **3b**, the Cp′ ring carbons are diastereotopic and six Cp′ resonances are observed: δ 14.2 (Cp*Me*) and 90.7, 91.5, 92.1, 93.8, 110.2 (Cp′). Again, only two sets of carbonyl resonances are recorded: δ 211.0 ($Fe(CO)_3$), 236.0 (μ-CO). The fact that only one resonance is observed for the $Fe(CO)_3$ carbonyl groups suggests rapid site exchange centered on *one* Fe atom. The terminal CO groups do not exchange with the μ-CO groups on the NMR time scale at room temperature. This finding is consistent with the observation that the activation energies for site exchanges on a single metal center are lower than those for intermetal site exchanges.[24]

Isomers **3** and **4** do not interconvert in solution at room temperature over a period of 1 week; thermolysis in refluxing toluene merely degrades the clusters to an insoluble brown powder within 3 h, although under 1700 psi of CO, isomer **3** is transformed into **4** at 150 °C.[25]

The reaction of $Cp_2W_2(CO)_4$ with $Fe_2S_2(CO)_6$ gives the W analogue, **4w**, of **4** in 5% yield along with a triangulo cluster, $Cp_2W_2Fe(\mu_3\text{-}S)(CO)_7$.[26] The W analogue of **4** (**4w**) has IR and NMR spectra completely comparable to those of the Mo cluster, and X-ray characterization shows that the crystals of **4w** and **4** are isomorphous.

(b) $Cp'_2Mo_2Co_2(CO)_4S_3$ (6). As pointed out in the Introduction, bis(μ-sulfido) functional groups may be used to construct metal sulfido clusters. We have utilized the compound $Cp_2Mo_2(\mu\text{-}S)_2(\mu\text{-}SH)_2$[20] (**5**, Cp′ = C_5H_4Me) to prepare a series of bimetallic, tetranuclear clusters. With $Co_2(CO)_8$, **5** reacts to give cluster **6** (eq 4). Interestingly, the complex $Cp_2Mo_2S_4$ reacts to give

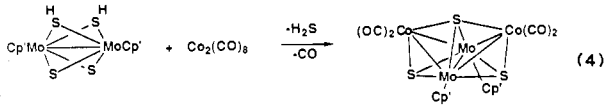

(4)

(6)

$Cp_2Mo_2Co_2(CO)_2S_4$,[15] a 60e *cubane* cluster. Apparently, the presence of the μ-SH groups in **5** permits a facile loss of sulfur as H_2S.

(c) $Cp'_2Mo_2Fe_2(CO)_6S_4$ (7). The synthesis and X-ray structure of **7** have been reported by Rakowski Dubois et al.[27] Their synthesis, from **5** and $Fe(CO)_5$ in the presence of Me_3NO, differs from ours (eq 5) but gives comparable yields. No reaction was

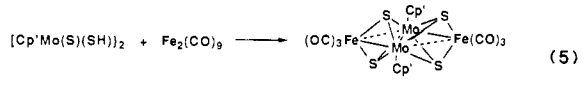

(5)

(7)

observed between **5** and $Fe_2(CO)_9$ in CH_2Cl_2 at room temperature. Presumably, the THF assists in the decomposition of the $Fe_2(CO)_9$ to give unsaturated carbonyl fragments, e.g. $Fe(CO)_4$·THF. The IR spectrum of **7** displays the two-band pattern characteristic of the a_1 + e CO stretching modes, and the ^1H NMR spectrum shows the presence of equivalent Cp′ groups.

An attempt was made to develop a higher yield preparation of complex **7** that involved the oxidation of **5** with I_2, followed by reaction of this product with $Na_2Fe_2(CO)_8$. The reaction of **5** with 1 equiv of I_2 gives an insoluble, black powder (possibly $Cp'_2Mo_2S_4I_2$ (**8**)). This complex reacted with $Na_2Fe_2(CO)_8$ to give a 25% yield of cluster **7**.

(d) $Cp'_2Mo_2Ni_2(CO)_2S_4$ (9). Nickel tetracarbonyl reacts with **5** to give cluster **9** (eq 6) in 25% yield. Cluster **9** displays CO stretching absorptions at 1990 and 1970 cm^{-1}, and the ^1H NMR spectrum shows the presence of equivalent Cp′ groups. The black solid gives green solutions in THF.

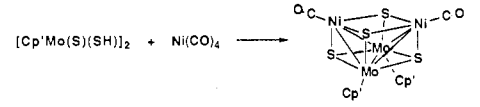

(6)

(9)

(e) $(Cp'Mo)_2(CpNi)_2S_4$ (10). $Cp_2Ni_2(CO)_2$ did not react with **5** at room temperature. In refluxing THF, low yields of olive green cluster **10**, small amounts of Cp_2Ni, and an unidentified brown cluster were formed (eq 7). The formula for **10**, $(Cp'Mo)_2(CpNi)_2S_4$, is conclusively derived from spectroscopic data and elemental analyses. The ^1H NMR spectrum shows equivalent Cp′ groups (δ 6.46, 2.52) and equivalent Cp groups (δ 4.11) in a 1:1 ratio. The parent ion was observed at m/z 726, as were fragments corresponding to sequential loss of all Cp′ and Cp groups.

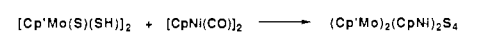

(7)

(10)

IR spectra indicated the absence of CO ligands and terminal M=S ligands. Single crystals of **10** suitable for X-ray analyses could not be obtained (very thin platelets were obtained in the best cases). If the bridging sulfide ligands donate 4e to the cluster, then **10** has a total of 68 valence-shell electrons (VSE), an electron count indicative of only two metal–metal bonds in the cluster bonding. Two possible electron-precise structures are shown below. Structures with delocalized M–M′ bonding are also possible, but we currently favor cubane structure III on the basis of the higher coordination number afforded the Ni atoms, the ubiquitous stability of cubane clusters, and the propensity of Mo to form Mo–Mo multiple bonds.

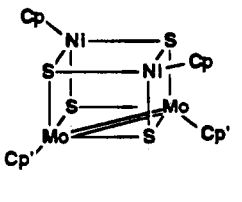

III

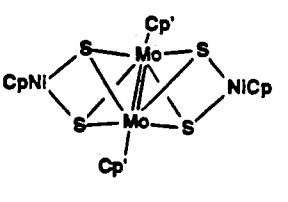

IV

Attempts to prepare clusters from **5** and $Cp_2Fe_2(CO)_4$ or $CpCo(CO)_2$ failed. No reaction was observed at room temperature, and at higher temperatures, **5** decomposed to intractable solids prior to any cluster-forming reactions.

Table II. Bond Distances (Å) in $Cp'_2Mo_2Fe_2(CO)_8S_2$ (**3b**)

	Cluster Core		
Mo–Mo′	2.821 (1)	Mo–Fe	2.776 (1)
Mo–Fe′	2.805 (1)	Mo–S	2.382 (1)
Mo–S′	2.343 (1)	Fe–S′	2.213 (2)
	Metal–Ligand[a]		
Mo–C1	2.391 (5)	Mo–C2	2.370 (5)
Mo–C3	2.318 (5)	Mo–C4	2.345 (6)
Mo–C5	2.358 (5)	Mo–CT	2.023
Mo–C7	2.025 (6)	Fe–C7	2.270 (6)
Fe–C8	1.775 (7)	Fe–C9	1.804 (7)
Fe–C10	1.799 (7)		

[a] CT = Cp centroid.

(23) (a) Braunstein, P.; Jud, J. M.; Tiripicchio, A.; Tiripicchio-Camellini, M.; Sappa, E. *Angew. Chem., Int. Ed. Engl.* **1982**, *21*, 307. (b) Braunstein, P.; Tiripicchio, A.; Camellini, M. T.; Sappa, E. *Inorg. Chem.* **1981**, *20*, 3586.
(24) Rosenberg, E.; Thorsen, C. B.; Milone, L.; Aime, S. *Inorg. Chem.* **1985**, *24*, 231.
(25) Bogan, L. E., Jr.; Rauchfuss, T. B.; Reingold, A. L. *J. Am. Chem. Soc.* **1985**, *107*, 3843.
(26) Curtis, M. D.; Williams, P. D. *J. Organomet. Chem.*, in press.
(27) Cowans, B.; Noordik, J.; Rakowski DuBois, M. *Organometallics* **1983**, *2*, 931.

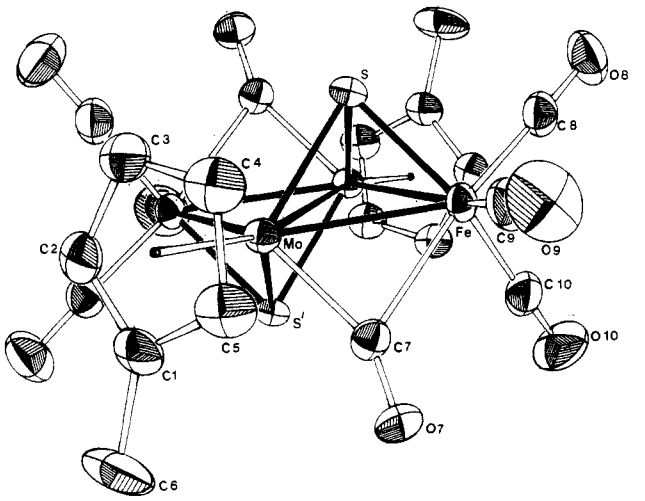

Figure 1. ORTEP plot with numbering scheme of $Cp'_2Mo_2Fe_2(CO)_8(\mu_3\text{-}S)_2$ (planar isomer, **3b**). Thermal ellipsoids are drawn at the 50% probability level.

Structures. (a) Mo–Fe–S Clusters. The structure of the butterfly cluster $Cp_2Mo_2Fe_2(CO)_8S_2$ (**4a**) was communicated by Braunstein et al.[23a] during the course of our work, and we became aware of Rakowski Dubois' independent synthesis and structure determination of $Cp'_2Mo_2Fe_2(CO)_6S_4$ (**7**) while we were in the midst of our own structure solution for this molecule. These workers kindly supplied us with atomic coordinates so we could compare the bond lengths and angles of **4a** and **7** to those of the clusters we had prepared and structurally characterized. Table II contains selected bond distances for **3b**.

Molecule **4a** has imposed C_2 symmetry (idealized C_{2v} symmetry). The four metal atoms have a "butterfly" arrangement with Mo at the hinge positions and Fe at the wing tips. The hinge angle is 104.1° and the FeFe distance (3.833 (5) Å) is nonbonding. The two μ_3-S atoms cap the exposed Mo_2Fe triangular faces (Mo–S ≃ 2.33 Å, Fe–S ≃ 2.16 Å). The Mo–Mo distance (2.85 Å) is only slightly longer than the Mo–Fe distance (2.82 Å) in spite of the fact that the covalent radius of Mo is some 0.13 Å greater than the radius of Fe.

In contrast, isomer **3b** lies on an inversion center (Figure 1), so that the Mo_2Fe_2 cluster core is strictly planar and the μ_3-sulfido ligands lie on opposite sides of the Mo_2Fe_2 plane. Two Mo–Fe bonds (2.776 (1) Å) are bridged by μ_2-CO ligands and the μ_3-S ligand, and two Mo–Fe bonds (2.805 (1) Å) are bridged only by the sulfur. The μ_2-carbonyl is asymmetrically bonded and seems to favor the Mo atom, as shown by the Mo–C–O angle, 152°, vs the Fe–C–O angle, 127°. As with **4a**, the Mo–Mo (2.821 (1) Å) and Mo–Fe bonds (average of 2.79 Å) are significantly closer in length than would be anticipated on the basis of the covalent radii of Mo and Fe.

Molecule **7** also has crystallographically imposed inversion symmetry, which results in a strictly planar Mo_2Fe_2 frame. This frame contains a very short Mo–Mo bond (2.62 Å) and two quite distinct Mo–Fe distances, one bonding, 2.85 Å, and one nonbonding, 3.61 Å. Four μ_3-sulfido ligands cap both sides of each Mo_2Fe triangle in a manner such that the sulfur atoms are nearly located over the nonbonding MoFe vector.

(b) $Cp'_2Mo_2Co_2(CO)_4S_3$ (6). A listing of bond distances is given in Table III. Figure 2 shows ORTEP plots of cluster **6** and the cluster core.

The structure of **6** is based on a butterfly arrangement of the metal atoms with the Mo atoms on the hinge axis and the Co atoms at the wing tips (hinge angle = 125°). An unusual μ_4-sulfido ligand caps the open edge of the butterfly (Co–S3 ≃ 2.24 Å, Mo–S3 ≃ 2.40 Å). The particular geometry of the μ_4-S ligand in **6** has been observed previously in certain Chevrel phases[28] and in several other clusters.[2b,e,29]

Table III. Bond Distances (Å) in $Cp'_2Mo_2Co_2(CO)_4S_3$ (**6**)

	Cluster Core		
Mo1–Co1	2.635 (1)	Mo1–Co2	2.635 (1)
Mo1–Mo2	2.646 (1)	Mo1–S1	2.362 (2)
Mo1–S2	2.362 (2)	Mo1–S3	2.390 (2)
Mo2–Co1	2.651 (1)	Mo2–Co2	2.656 (1)
Mo2–S2	2.351 (2)	Mo2–S1	2.354 (2)
Mo2–S3	2.402 (2)	Co1–S1	2.199 (2)
Co1–S3	2.239 (2)	Co2–S2	2.194 (2)
Co2–S3	2.234 (2)		
	Metal–Ligand[a]		
Co1–C1	1.758 (7)	Co1–C2	1.774 (7)
Co2–C3	1.761 (8)	Co2–C4	1.766 (7)
Mo1–C5	2.338 (7)	Mo1–C6	2.364 (7)
Mo1–C7	2.363 (7)	Mo1–C8	2.329 (6)
Mo1–C9	2.341 (7)	Mo1–CT1	2.018
Mo2–C11	2.356 (6)	Mo2–C12	2.339 (7)
Mo2–C13	2.326 (7)	Mo2–C14	2.340 (7)
Mo2–C15	2.349 (6)	Mo2–CT2	2.016

[a] CT = Cp centroid.

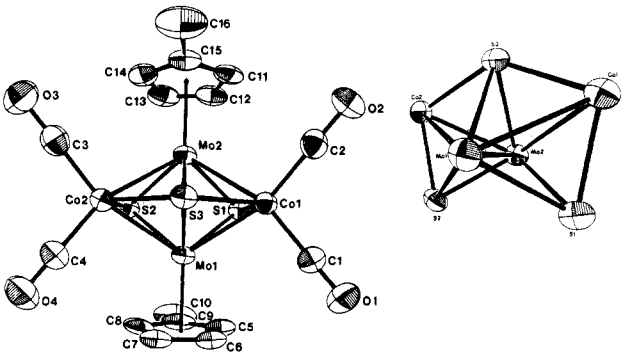

Figure 2. ORTEP plot with numbering scheme of $Cp'_2Mo_2Co_2(CO)_4(\mu_3\text{-}S)_2(\mu_4\text{-}S)$ (**6**). Thermal ellipsoids are drawn at the 50% probability level. The inner core is shown at right.

Two μ_3-sulfido ligands cap each Mo_2Co triangular face (Co–(μ_3-S) ≃ 2.20 Å, Mo–(μ_3-S) ≃ 2.36 Å). Note that these M–S distances reflect the expected difference (ca. 0.16 Å) between the covalent radii of Mo and Co. In contrast, the Mo–Mo distance (2.646 (1) Å) is equal to the mean of the Mo–Co distances in the cluster core. This relative contraction of the Mo–Mo distance was noted in the Mo–Fe–S clusters disussed above. Furthermore, the Mo–Co distances (2.63–2.66 Å) in **6** are contracted by ca. 0.1 Å when compared to Mo–Co bond lengths of 2.74–2.76 Å in the related compounds $CpMoCo_3(CO)_{11}$,[30] $CpMoCoFe(\mu_3\text{-}S)(CO)_7(PR_3)$,[31] and $CpMoCo_2Fe(\mu_3\text{-}S)(CO)_{10}(\mu\text{-}AsMe_2)$.[32]

In contrast to the bonding in the other clusters prepared in this work, the bonding in cluster **6** cannot be described in electron-precise terms. The S 3s orbital is probably too low in energy to contribute substantially to the bonding; therefore, each sulfur atom can donate only 4e to the cluster framework. The total VSE count is then 60, apropos of a closo tetrahedron if the bonding were electron precise. The electron deficiency is also obvious from the fact that the μ_4-S ligand must form four bonds with only three atomic orbitals ($3p_{x,y,z}$). A simplistic rationalization of the observed structure may be made with cluster counting rules[33] *provided* one assumes that the Mo atoms use only three atomic orbitals for

(28) Potel, M.; Chevrel, R.; Sergent, M.; Armici, J. C.; Deroux, M.; Fischer, O. *J. Solid State Chem.* **1980**, *35*, 286.

(29) (a) Pasynskii, A. A.; Eremenko, I. L.; Ellert, O. G.; Novoturtsev, V. M.; Rakitin, Y. V.; Kalinnikov, V. T.; Shklover, V. E.; Struchov, Y. T. *J. Organomet. Chem.* **1982**, *234*, 315. (b) Ghilardi, C. A.; Midollini, S.; Sacconi, L. *J. Chem. Soc., Chem. Commun.* **1981**, *47*.

(30) Schmid, G.; Bartl, K.; Boese, R. *Z. Naturforsch., B: Anorg. Chem., Org. Chem.* **1977**, *32B*, 1277.

(31) Richter, F.; Vahrenkamp, H. *Angew. Chem., Int. Ed. Engl.* **1980**, *19*, 65.

(32) Richter, F.; Muller, M.; Gartner, N.; Vahrenkamp, H. *Chem. Ber.* **1984**, *177*, 2438.

(33) (a) Wade, K. In *Transition Metal Clusters*; Johnson, B. F. G., Ed.; Wiley: New York, 1980; pp 193–264. (b) Rudolph, R. W. *Acc. Chem. Res.* **1976**, *9*, 446. (c) Johnson, B. F. G.; Lewis, J. *Adv. Inorg. Chem. Radiochem.* **1981**, *24*, 225.

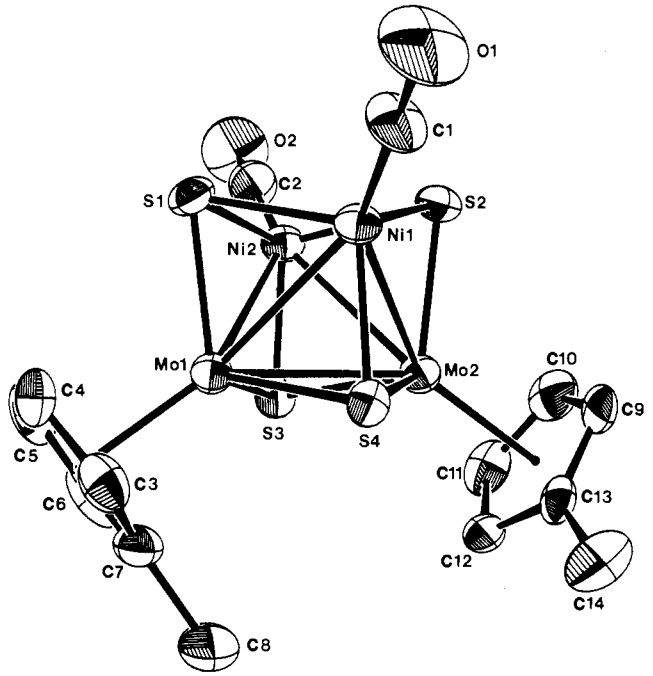

Figure 3. ORTEP plot with numbering scheme of $Cp'_2Mo_2Ni_2(CO)_2(\mu_3\text{-}S)_4$ (**9**). Thermal ellipsoids are drawn at the 50% probability level.

Table IV. Bond Distances (Å) in $Cp'_2Mo_2Ni_2(CO)_2S_4$ (**9**)

	Cluster Core		
Mo1–Mo2	2.829 (1)	Mo1–Ni1	2.723 (1)
Mo1–Ni2	2.720 (1)	Mo1–S1	2.252 (3)
Mo1–S3	2.328 (2)	Mo1–S4	2.329 (2)
Mo2–Ni1	2.724 (1)	Mo2–Ni2	2.721 (2)
Mo2–S2	2.262 (3)	Mo2–S3	2.332 (2)
Mo2–S4	2.325 (2)	Ni1–S1	2.278 (3)
Ni1–S2	2.288 (3)	Ni1–S4	2.162 (3)
Ni2–S1	2.286 (3)	Ni2–S2	2.282 (3)
Ni2–S3	2.158 (3)		
	Metal–Ligand[a]		
Mo1–C3	2.36 (1)	Mo1–C4	2.37 (1)
Mo1–C5	2.36 (1)	Mo1–C6	2.34 (1)
Mo1–C7	2.36 (1)	Mo1–CT1	2.04
Mo2–C9	2.37 (1)	Mo2–C10	2.36 (1)
Mo2–C11	2.35 (1)	Mo2–C12	2.35 (1)
Mo2–C13	2.40 (1)	Mo2–CT2	2.05
Ni1–C1	1.75 (1)	Ni2–C2	1.75 (1)

[a] CT = Cp centroid.

cluster framework bonding. The CpMo group contributes 6 + 5 − 12 = −1e to the cluster framework, and the $Co(CO)_2$ fragment contributes 4 + 9 − 12 = 1e.[33a] With each sulfur atom contributing four electrons, there are then twelve cluster framework electrons or six cluster framework *pairs* ($S = 6$). There are seven vertices (N) in **6**, so that $S = N - 1$ and a bicapped pentagonal bipyramid is predicted.[33c] This model fails to account for the high connectivity (six framework bonds) around the Mo atom, however. An EHMO description of the bonding in **6** will be given elsewhere.

(c) $Cp'_2Mo_2Ni_2(CO)_2S_4$ (9). Bond distances for **9** are in Table IV, and an ORTEP plot is shown in Figure 3. The structure of **9** may be described as having an Mo_2Ni_2 butterfly core with Mo atoms on the hinge axis (hinge angle = 101°) and Ni atoms at the wing tips. There are five metal–metal bonding contacts (Mo–Mo = 2.83 Å, Mo–Ni ≃ 2.72 Å) and one nonbonding, or very weakly bonding,[34,35] Ni–Ni distance (2.96 Å), as expected for a 62-VSE count.

Due to the placement of the μ_3-sulfido ligands, the cluster may also be described as a C_{2v}-symmetry cubane. Molecular orbital descriptions of the M_4X_4 cubanes are well developed and provide a good rationale of cluster structure with the VSE count.[36] In homometallic cubanes, the 60-VSE clusters typically have six M–M bonds and idealized T_d symmetry. Clusters with higher or lower VSE counts often show D_{2d} or D_2 Jahn–Teller distortions as a result of populating degenerate orbitals associated with highly delocalized M–M bonding. In the lower symmetry heteronuclear clusters, e.g., **9**, the "extra" 2e are apparently localized in a Ni–Ni antibonding orbital, and only this bond is elongated.

The metal–sulfur distances in **9** show an interesting pattern. The Mo–S bonds (Mo1–S1, Mo2–S2) involving the sulfur atoms that cap the $MoNi_2$ faces have an average length of 2.26 Å, whereas the Mo–S bonds (Mo1–S3, Mo2–S4) involving those sulfur atoms that cap the Mo_2Ni faces have an average length of 2.33 Å. The latter value is normal for single bonds between Mo and bridging sulfur atoms. The former value falls between the single-bond distances and the typical Mo=S double-bond distance, 2.14 Å.[16] This pattern of bond lengths undoubtedly reflects the fact that the energies of the atomic orbitals of Mo and S are well matched for π-bonding.

Mo–Mo Bond Lengths. The relative shortness of the Mo–Mo bonds in the clusters described above was noted several times. The Mo–Mo bond contraction in **6** and **7** is so severe that these bonds are shorter than those observed in compounds with formal Mo=Mo double bonds.[37]

Table V lists a number of dinuclear Mo complexes ranked according to the number of bridging S atoms regardless of the formal oxidation state of Mo, the connectivity of the S atom (μ_2-, μ_3-, μ_4-S; μ-SR), and the nuclearity of the complex (dimer or cluster).

It is apparent that with one bridging sulfur, the Mo–Mo distance is ≳3.0 Å, a distance common for Mo–Mo single bonds in organometallic compounds. With two bridging S atoms, the Mo–Mo bond shrinks to an average distance of 2.87 [4] Å. The average distance in the nine compounds listed with four bridging S atoms is 2.60 [1] Å.[38]

Table V. Correlation of Mo–Mo Bond Length with Number of Bridging Sulfur Atoms

no. of μ-S	compd	Mo–Mo, Å	formal Mo oxidn state	ref
1	$Cp_3Mo(\mu_3\text{-}S)(CO)_6^+$	3.09	II	22
	$Cp_2Mo_2(CO)_3(\mu\text{-}SC(Me)SEt)$	3.163	II	49
2	$Cp_2Mo_2O_2(\mu\text{-}S)_2$	2.894	V	50
	$Cp'_2Mo_2O_2(\mu\text{-}S)_2$	2.904	V	16a
	$Cp'_2Mo_2S_2(\mu\text{-}S)_2$	2.881	V	16a
	$Cp^*_2Mo_2S_2(\mu\text{-}S)_2$[a]	2.905	V	16a
	$Cp_3Mo_3(\mu\text{-}S)_3(\mu_3\text{-}S)^+$	2.812	IV	51
	$(i\text{-}PrCp)_4Mo_4(\mu_3\text{-}S)_4$	2.904	III	52
	$Cp'_2Cp^*_2Mo_4(\mu_3\text{-}S)_4$	2.902	III	36
	$Cp_2Mo_2(CO)_2(\mu\text{-}SCMe)(\mu\text{-}SEt)$	2.806	III	49
3	$Cp_2Mo_2(\mu\text{-}SMe)_3^+$	2.785	III	38
4	$Cp_2Mo_2(\mu\text{-}SC_3H_6S)_2^+$	2.599	3.5	16b
	$Cp'_2Mo_2(\mu\text{-}S_2CH_2)(\mu\text{-}SC_2H_2S)$	2.601	III	53
	$Cp'_2Mo_2(\mu\text{-}S_2CH_2)(\mu\text{-}SCH_3)_2$	2.596	III	53
	$Cp^*_2Mo_2(\mu\text{-}S)_2(\mu\text{-}S_2)$[a]	2.599	IV	10a
	$Cp'_2Mo_2(\mu\text{-}S)(\mu\text{-}SCH_3)(\mu\text{-}S_2CH_2)^+$	2.610	IV	54
	$Cp_2Mo_2(\mu\text{-}S)_2(\mu\text{-}SMe)_2$	2.582	IV	55
	$(\pi\text{-}PhMe)_2Mo_2(\mu\text{-}SMe)_4^{2+}$	2.614	III	56
	$Cp_2Mo_2(\mu\text{-}SMe)_4^{n+}$			
	$n = 0$	2.603	III	57
	$n = 1$	2.617	3.5	57

[a] $Cp^* = C_5Me_5$.

(34) Ghilardi, C. A.; Midollini, S.; Sacconi, L. *Inorg. Chim. Acta* **1978**, *31*, L431.
(35) Vahrenkamp, H.; Uchtmann, V. A.; Dahl, L. F. *J. Am. Chem. Soc.* **1968**, *90*, 3272.
(36) Williams, P. D.; Curtis, M. D. *Inorg. Chem.* **1986**, *25*, 4562.
(37) Curtis, M. D.; Messerle, L.; D'Errico, J. J.; Solis, H. E.; Barcelo, I. D.; Butler, W. M. *J. Am. Chem. Soc.* **1987**, *109*, 3603.
(38) Exceptions to the correlation presented here occur when there is a formal M=M double bond and when the coordination number and geometry of the two molybdenum atoms differ markedly. See Table IV in: Gomes de Lima, M. B.; Guerchais, J. E.; Mercier, R.; Petillon, F. Y. *Organometallics* **1986**, *5*, 1952.

Table VI. Cyclic Voltammetry of the $M_2M'_2S_{2-4}$ Clusters[a,b]

compd	E_{red}, V[c]	ΔE_p, mV	i_{pa}/i_{pc}[d]	E_{ox}, V[c]	ΔE_p, mV	i_{pc}/i_{pa}[d]
$Cp'_2Mo_2Fe_2(CO)_8S_2$ (**4b**)	−1.31	540	nr	+0.60	irr	
(butterfly isomer)	−1.65	50	nr	+0.97	irr	
$Cp'_2Mo_2Fe_2(CO)_8S_2$ (**3b**)	−1.09	640	nr	+0.58	irr	
(planar isomer)	−1.55	70	nr	+0.98	irr	
$Cp_2W_2Fe_2(CO)_8S_2$ (**4w**)	−1.36	430	nr	+0.26	60	0.8
(butterfly isomer)	−1.63	60	nr	+0.67	irr	
$Cp'_2Mo_2Fe_2(CO)_6S_4$ (**7**)	−1.38	60[e]	nr	+0.19	290	0.7
	−1.56	50	nr			
	−1.72	80	nr			
$Cp'_2Mo_2Co_2(CO)_4S_3$ (**6**)	−1.40	30	0.9	−0.03	irr	
	−1.74	220	1.0	+0.27	irr	
$Cp'_2Mo_2Ni_2(CO)_2S_4$ (**9**)	−1.58	50	0.9	−0.11	irr	
	−2.11	50	0.8	+0.09	irr	
$(Cp'Mo)_2(CpNi)_2S_4$ (**10**)	−1.40	50	0.8	−0.48	50	1.0
	−2.23	irr		−0.02	50	1.0

[a] 0.10 M Et_4NBF_4 in CH_3CN; sweep rates between 25 and 200 mV/s; 0.10 M $AgNO_3$/Ag reference; all samples less than 1 mM in cluster. [b] Cp_2Fe/Cp_2Fe^+ internal standard; $E_{p/2}$ = +0.07 V vs Ag/Ag^+. [c] $E_{p/2}$ is given unless wave is irreversible (irr), in which case E_p is given. [d] Peak current ratio not reported when waves are irreversible or when resolution did not allow accurate determination (nr). [e] Two anodic counterwaves (both dependent on the initial reduction) were observed (see text). $E_{p/2}$ value reported is based on the first oxidation.

The sulfido clusters follow much the same pattern: **3**, **4**, and **9** (two μ-S) have Mo–Mo distances of 2.82–2.85 Å, while **6** and **7** (three and four μ-S, respectively) have Mo–Mo distances of 2.65 and 2.62 Å, respectively. The bond contraction in **6** is greater than that displayed by $Cp_2Mo_2(\mu\text{-}SMe)_3^+$, the only other molecule of the type under consideration here with three bridging S atoms. The enhanced bond contraction in **6** may be related to the delocalized bonding in this "electron-deficient" cluster.

A rationale for the Mo–Mo bond length independence of the Mo oxidation state in compounds of the type $R_2Mo_2(\mu\text{-}SR')_{4-x}(\mu\text{-}S)_x$ (R = aryl, Cp) is readily derived from the EHMO scheme for these molecules presented by Rakowski DuBois et al.[39] This calculation orders the M–M frontier orbitals in the sequence $\sigma < \delta^* < \delta$. The orbital occupation for the various oxidation states (in parentheses) are then as follows: $(\mu\text{-}S)_4Mo_2$ (V), σ^2; $(\mu\text{-}S)_2(\mu\text{-}SR)_2Mo_2$ (IV), $\sigma^2\delta^{*2}$; $(\mu\text{-}SR)_4Mo_2$ (III), $\sigma^2\delta^{*2}\delta^2$. Since occupation (or lack thereof) of the δ and δ^* orbitals has little effect on the metal–metal bond strength, the Mo–Mo distance is independent of the formal oxidation state of the metal. The above rationale does not explain why the Mo–Mo bond is short to begin with. However, this same EHMO analysis shows that the unoccupied M–M π-bonding orbitals of the Cp_2M_2 fragment are used to construct the molecular orbitals for M–S bonding and thus become occupied in the S-bridged complex. As the number of μ-S ligands increases, the electron occupation of orbitals that are also M–M bonding increases and the M–M distance decreases. This type of argument, utilizing major contributions from metal s and p orbitals in the M–M and M–S bonding instead of d orbitals, has been published by Fenske et al.[40] It is interesting to note that the increase in the Mo–Mo bond length upon 1e oxidation of $Cp_2Mo_2(SR)_4$, 2.603 (2) → 2.617 (4) Å (Table V), is consistent with removal of a weakly bonding electron and supports the $\sigma < \delta^* < \delta$ ordering of orbitals in Rakowski DuBois' EHMO[39] calculation.

Cyclic Voltammetry. The clusters prepared in this study are extremely robust as a consequence of the presence of nonlabile Cp- and face-capping sulfido ligands. These features should prevent electrochemical degradation and stabilize multiple oxidation states.[1,41]

The results of our cyclic voltammetry experiments are summarized in Table VI. The reported potentials were independent of the scan rates employed (25–200 mV/s).

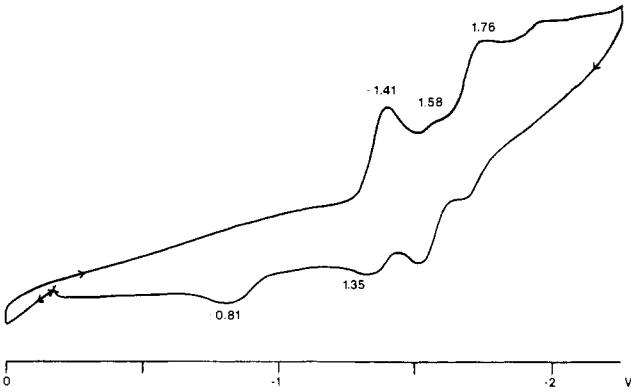

Figure 4. Cyclic voltammogram of $Cp'_2Mo_2Fe_2(CO)_6(\mu_3\text{-}S)_4$ (**7**) (scan rate = 100 mV/s, X = sweep origin).

Scheme I. Proposed ECE Mechanism for Reduction of Clusters **3** and **4**

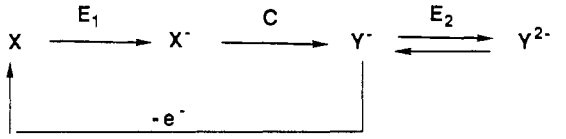

Reduction of the $M_2Fe_2S_2$ Clusters (3b, 4b, 4w). The observed voltammogram for the planar cluster $Cp_2Mo_2Fe_2(CO)_8S_2$ (**3b**) is typical for all the $M_2Fe_2S_2$ clusters investigated (supplementary Figure 6). In every case, an irreversible 1e reduction precedes and merges with a second, reversible 1e wave. The reversibility of the second wave was demonstrated by starting the voltage sweep at the cathodic side of the wave, reversing the sweep at a point just past the reoxidation wave, and varying the sweep rate (supplementary Figure 7). At high sweep rates, the 2−/1− couple is cleanly reversible (ΔE_p = 70 mV, $i_a/i_c \simeq 1.0$). At low sweep rates, the neutral species in the bulk solution has time to diffuse to the electrode surface, and a small 0/1− peak appears at −1.41 V as a shoulder on the 1−/2− wave.

The reduction behavior of these clusters is adequately described by an ECE mechanism[42] (Scheme I) in which the neutral cluster, X, is reduced in the first wave to X^-. The species X^- undergoes a rapid chemical transformation to a new species Y^-. The latter then undergoes a reduction (E_2) to Y^{2-}. On the anodic return sweep, Y^{2-} is reversibly reoxidized to Y^-. Species Y^- is more stable than X^-, and consequently, a larger potential (E_3) is required to reoxidize Y^- to X^0. We have not been able to establish a quan-

(39) DuBois, D. L.; Miller, W. K.; Rakowski DuBois, M. *J. Am. Chem. Soc.* **1981**, *103*, 3429.
(40) (a) Rives, A. B.; Xiao-Zeng, Y.; Fenske, R. F. *Inorg. Chem.* **1982**, *21*, 2286. However, Wooley and Evans have argued that metal d orbitals, not s and p, are most important in metal–metal bonding: (b) Wooley, R. G. *Inorg. Chem.* **1985**, *24*, 3519, 3525. (c) Evans, D. G. *Ibid.* **1986**, *25*, 4602.
(41) Lemoine, P. *Coord. Chem. Rev.* **1982**, *47*, 55.
(42) Bard, A. J.; Faulkner, L. R. *Electrochemical Methods: Fundamentals and Applications*; Wiley: New York, 1980; Chapter 3.

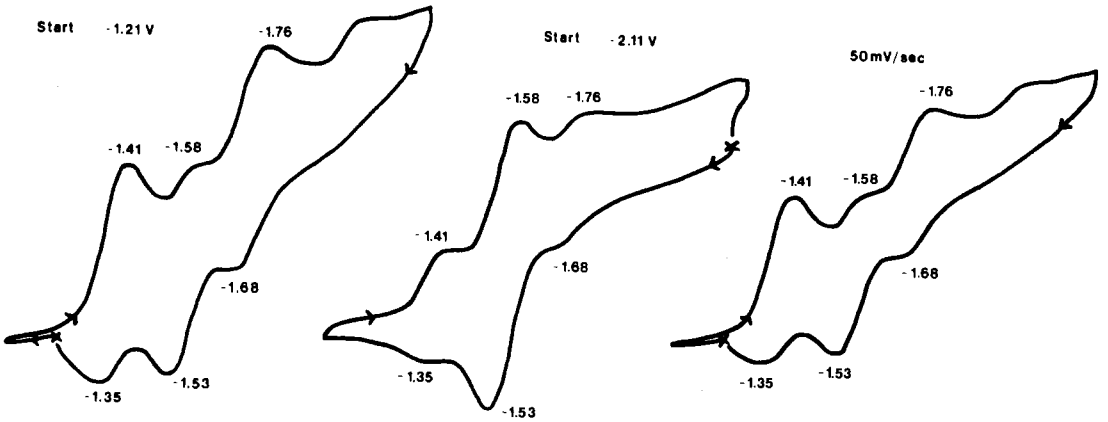

Figure 5. Effects of starting potential and scan rate on current amplitudes in cyclic voltammograms of 7: scan rate = 200 mV/s (left and middle), 50 mV/s (right); starting potential = −1.21 V (left and right), −2.11 V (middle).

Scheme II. Proposed Mechanism for the Reduction of Cluster 7[a]

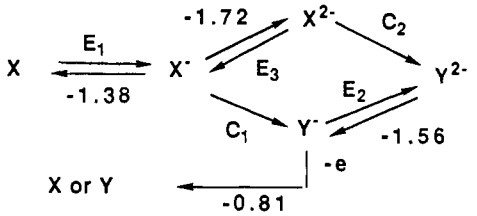

[a] Indicated potentials are $E_{p/2}$.

titative rate constant for the chemical step (C) in the ECE mechanism because of the poor resolution of the two cathodic waves. However, the rapidity of chemical step C suggests a minimal structural reorganization during the transformation.

Reduction of $Cp'_2Mo_2Fe_2(CO)_6S_4$ (7). The reduction of **7** was previously reported to display a reversible reduction at $E_{p/2} = -1.06$ V and a "quasi-reversible" reduction at $E_{p/2} = -1.47$ V (vs SCE) with a $\Delta E_p = 180$ mV for the second reduction process.[27] We observe a much more complex reduction profile (Figure 4) that suggests the presence of at least *three* redox couples.

The first reduction peak at −1.41 V is coupled to an oxidation peak at −1.35 V and *another* peak at −0.81 V. Two further redox waves were observed at lower potentials. The relative current amplitudes, i_a/i_c, of these waves were dependent on both the scan rate and starting potential of the voltammogram (Figure 5). All the initial reduction waves seem to be coupled reversibly ($\Delta E_p \leq 80$ mV) to oxidation waves. We propose the mechanism shown in Scheme II to explain the anomalous current ratios.

The cluster is reduced at $E_{p/2} = -1.38$ V to X^-, which can rearrange via chemical step C_1 to Y^-, or at the appropriate potential, a more rapid electrochemical step (E_3, −1.76 V) reduces most of the X^- generated in the first reduction to X^{2-} when the scan rate is ≥50 mV/s. The small amount of Y^- generated by C_1 is reduced reversibly to Y^{2-} at potential E_2 ($E_{p/2} = -1.56$ V).

Since the rate of step C_1 is comparable to the scan rate, the current ratios, i_a/i_c, of the E_2 and E_3 waves should be dependent on the scan rate. As Figure 5 shows, the reduction wave associated with E_2 increases as the scan rate is lowered, and there is more time for Y^- to form via step C_1.

Chemical step C_2 (Scheme II) is proposed to be relatively fast compared to the switching time at the electrode, so that most of the X^{2-} formed by reduction E_3 is converted into Y^{2-}. Therefore, on the return sweep there is a large anodic wave at −1.53 V corresponding to the Y^{2-}/Y^{1-} couple E_2. Subsequent small anodic waves are observed at −1.35 V (X^{1-}/X^0, E_1) and at −0.81 V (Y^{1-}/X^0). Slow scan rates should enhance the current due to E_2 at the expense of both E_1 and E_3, and this is observed (Figure 5). In addition, starting the voltammogram at cathodic potentials (where the primary species in the electrode surface layer is Y^{2-}) nearly extinguishes the E_1 and E_3 wave as expected (E_1 and E_3 cannot be completely quenched due to diffusion of neutral X from the bulk into the electrode boundary layer).

Scheme III. Proposed Mechanism for Reduction of Cluster 6

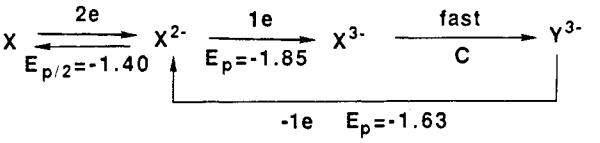

Although the identification of the species Y awaits further work, an intriguing possibility is that Y is the cubane isomer of **7**. The 2e-reduction product of **7** has a 68-VSE count, the same as $(Cp'Mo)_2(CpNi)_2S_4$ (**10**), for which a cubane structure was proposed above. Actually, the conversion of the planar structure of **7** to a cubane involves minimal structural reorganization—a folding of the Fe_2Mo_2 rhombus with a concomitant rotational slip of the sulfides as shown in eq 8.

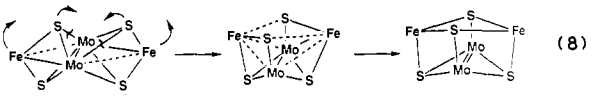

$Cp'_2Mo_2Co_2(CO)_4S_3$ (6). The electrochemistry of **6** is apparently complicated by an electrode-surface reaction. When the voltammogram is started at −0.20 V, a very small, anodic wave at −0.35 V and a completely irreversible cathodic wave at −1.03 V are observed. The currents associated with these peaks are too small to be attributed to a Faradaic process and depend on the amount of time the electrode is held at −0.20 V.

Starting the reduction sweep at −0.70 V completely eliminates these spurious peaks and produces a well-defined, reversible 2e-reduction peak ($\Delta E_p = 30$ mV) with $E_{p/2} = -1.40$ V (peak A), followed by another cathodic wave at −1.85 V (peak B). Peak B is coupled to an anodic wave at −1.63 V ($i_a/i_c = 1.0$). This behavior may be accommodated by the EEC type mechanism shown in Scheme III.

$Cp'_2Mo_2Ni_2(CO)_4S_4$ (9) and $(Cp'Mo)_2(CpNi)_2S_4$ (10). In contrast to the complex behavior displayed by the clusters discussed above, both **9** and **10** show fairly simple electrochemistry. Cluster **9** has two 1e-reduction waves, both fully reversible, at −1.58 and −2.11 V. Two irreversible oxidation processes are observed at −0.11 and +0.09 V.

Cluster **10** exhibits two reversible 1e oxidations at 0.48 and −0.02 V, one reversible 1e reduction at −1.40 V, and one irreversible reduction at −2.23 V. Thus, the 62-VSE cluster, **9**, is more easily reduced, and the electron-rich 68-VSE cluster, **10**, is more readily oxidized.

Conclusions

Reaction of the metal–metal triple bond in $Cp_2M_2(CO)_4$ type complexes with dinuclear sulfido complexes represents a new method of controlled cluster assembly. This method is similar to that for the reaction of dinuclear sulfido complexes with com-

pounds containing labile carbonyl ligands. These two methods afford, in particular, a convenient route to interesting clusters that incorporate group 6 metals (Mo or W) and group 8–10 metals (Fe, Co, Ni). These clusters may resemble the active site of "sulfided" iron, cobalt, and nickel molybdate hydrotreating catalysts. The Mo–Mo bond lengths in these clusters and in related dinuclear complexes contract as the number of μ-sulfido ligands increases. These clusters also exhibit a rich electrochemistry involving structural reorganizations as the cluster core is reduced.

Experimental Section

All reactions and manipulations were performed under prepurified nitrogen atmosphere by using standard Schlenk techniques unless noted otherwise. Solid products were typically air stable and were handled in air during the short times required for transferring and weighing.

Reagent grade solvents were dried and distilled under nitrogen prior to use. Hexanes were distilled from CaH_2. Dichloromethane was predried over $CaCl_2$ and distilled from P_2O_5. Toluene and THF were distilled from Na/benzophenone.

NMR spectra were obtained on a Varian T60A spectrometer. Mass spectra of solid samples were obtained by thermal desorption from the solids probe of a Finnegan GC/MS. Visible spectra were obtained on a Cary 219 UV–vis spectrometer. Elemental analyses were obtained from Galbraith (Knoxville, TN), Spang (Eagle Harbor, MI), or Schwarzkopf (Woodside, NY) Microanalytical Laboratories.

The compound $Fe_2(\mu\text{-}S_2)(CO)_6$ (**2**) was prepared by the modification as reported by Seyferth et al.[43] A more efficient version of this synthesis has been reported recently by Rauchfuss et al.[44]

Synthesis of $Cp'_2Mo_2Fe_2(\mu_3\text{-}S)_2(CO)_8$ (Isomers 3 and 4). A solution of 1.22 g (2.64 mmol) of $Cp'_2Mo_2(CO)_4$ (Mo≡Mo)[45] in 15 mL of toluene was added dropwise to a stirred solution of 0.46 g (1.32 mmol) of $Fe_2(\mu\text{-}S_2)(CO)_6$ (**2**) in 20 mL of hexane/toluene (3:1 v/v) (the 2:1 ratio of Mo dimer to Fe dimer is dictated by the stoichiometry shown in eq 3). The solution rapidly turned dark brown, yielding a brown mixture of crystalline **3b** and **4b**. The most efficient method of obtaining the pure clusters proved to be elution chromatography. Elution of all the reaction solids on a column of activated alumina powder (45 × 3 cm) gave the following fractions: light orange $Fe_3(\mu_3\text{-}S)_2(CO)_9$ (hexane), red $(MeCp)_2Mo_2(CO)_6$ (1:1 hexane/toluene), purple-brown **3b** (toluene), and red-brown **4b** (CH_2Cl_2). Removal of the solvents gave the corresponding solid compounds, which were recrystallized from CH_2Cl_2/hexane. **3b**: 0.15 g, 15%; mp 188 °C. **4b**: 0.62 g, 63%; mp 222 °C. Anal. Calcd for $(MeCp)_2Fe_2(\mu_3\text{-}S)_2(CO)_8$ (**4b**) ($C_{29}H_{14}Fe_2Mo_2O_8S_2$): C, 32.03; H, 1.88; Fe, 14.89; Mo, 25.58; S, 8.55. Found: C, 32.06; H, 1.95; Fe, 15.87; Mo, 25.20; S, 8.74.

The analogous Cp-containing clusters (**3a**, **4a**) were obtained in identical fashion from $Cp_2Mo_2(CO)_4$.

Synthesis of $Cp'_2Mo_2Fe_2(\mu_3\text{-}S)_4(CO)_6$ (7). (A) A 100-mL side-arm flask was charged with 0.36 g (1.0 mmol) of $Fe_2(CO)_9$ and 0.48 g (1.0 mmol) of $CpMo(S)_2(SH)_2$ (**5**). The solids were partially dissolved in 50 mL of THF, and the mixture was stirred for 2 h, during which time the golden flakes of $Fe_2(CO)_9$ disappeared and the solution color changed from violet to brown. The solution was concentrated to a 10-mL volume and transferred onto a column of alumina (40 × 3 cm). The initial green band was collected by using CH_2Cl_2 as eluant. The solvent was removed from the collected fraction to yield dark green crystalline solid **7**: yield 0.15 g (20%); mp 305 °C. Anal. Calcd for $Cp_2Mo_2Fe_2(\mu_3\text{-}S)_4(CO)_6$ ($C_{18}H_{14}Fe_2Mo_2O_6S_4$): C, 28.52; H, 1.86; S, 16.91. Found: C, 28.44; H, 1.81; S, 16.18.

(B) Iodine (0.36 g, 1.42 mmol) dissolved in 20 mL of CH_2Cl_2 was added dropwise to 0.20 g (0.71 mmol) of **5** in 20 mL of CH_2Cl_2. The mixture rapidly turned black and was filtered to give a black powder and a dilute red-brown filtrate. The black powder was dissolved in 100 mL of warm THF to give a deep green solution. This solution was added by dropping funnel to 0.27 g (0.71 mmol) of $Na_2Fe_2(CO)_8$ in 20 mL THF at −20 °C. The initial brown color of the mixture became green-brown as the addition was completed. Small white crystals (NaI?) were observed in the mixture. The mixture was warmed to room temperature and then rapidly filtered through 8 cm of alumina. An initial emerald green fraction was collected while brown and purple fractions remained irreversibly adsorbed on the alumina. The THF was removed from the green solution under vacuum to give dark green solid **7**, which was recrystallized from CH_2Cl_2/hexane: yield 0.14 g (25%).

Synthesis of $Cp'_2Mo_2Co_2(\mu_3\text{-}S)_2(\mu_4\text{-}S)(CO)_4$ (6). A 35-mL solution of $Co_2(CO)_8$ (0.36 g, 1.0 mmol) in toluene was added dropwise to a stirred slurry of **5** (0.50 g, 1.0 mmol) in 10 mL of toluene. Stirring was continued at room temperature for 2 h to give a deep brown solution. The reaction mixture was reduced in volume to 30 mL under vacuum and placed on a chromatography column packed with Florisil (60–100 mesh, 60 × 3 cm). Elution with hexane/toluene (4:1 v/v) gave an initial black band that was collected and stripped of solvent in vacuo to yield black crystalline **6**. The product could be recrystallized from CH_2Cl_2/hexane at −78 °C: yield 0.35 g (50%); mp 177 °C. Anal. Calcd for $Cp'_2Mo_2Co_2(\mu_3\text{-}S)_2(\mu_4\text{-}S)(CO)_4$ ($C_{16}H_{14}Co_2Mo_2O_4S_3$): C, 28.42; H, 2.09; S, 14.22. Found: C, 28.76; H, 2.01; S, 14.41.

Synthesis of $Cp'_2Mo_2Ni_2(\mu_3\text{-}S)_4(CO)_2$ (9). A tared 100-mL side-arm flask, cooled to −196 °C, was connected to a cylinder of $Ni(CO)_4$, and $Ni(CO)_4$ (0.43 g, 2.5 mmol) was condensed into the flask. The flask was allowed to warm to room temperature after 10 mL of THF had been added through a septum cap. This solution was transferred by cannula to another 100-mL flask that contained a slurry of 0.48 g (1.0 mmole of **5** in 10 mL of THF. The color of the resulting mixture changed from purple to black after 2 h at ambient temperature. Stirring was continued for several hours, after which the solvent was removed. The CH_2Cl_2-soluble portion of this solid was transferred to an alumina column (35 × 2 cm) and eluted with CH_2Cl_2. An initial pine green band was collected and stripped of solvent to leave dark green, crystalline **9**: yield 0.16 g (25%); mp >350 °C. Anal. Calcd for $Cp'_2Mo_2Ni_2(\mu_3\text{-}S)_4(CO)_2$ ($C_{14}H_{14}Mo_2Ni_2O_2S_4$): C, 25.80; H, 2.16; Mo, 29.44; Ni, 18.01; S, 19.67. Found: C, 26.65; H, 2.34; Mo, 28.40; Ni, 17.68; S, 19.73.

Synthesis of $(Cp'Mo)_2(CpNi)_2S_4$ (10). A 100-mL side-arm flask was charged with 0.32 g (1.0 mmol) of $Cp_2Ni_2(CO)_2$ and 0.50 g (1.0 mmol) of **5**. The solids were dissolved in 50 mL of THF to give a reddish brown solution. Heating the mixture to reflux was accompanied by significant evolution of gas with a fairly rapid color change to a dark green-brown solution. After being refluxed for 1.5 h, the mixture was cooled to room temperature and filtered to yield 0.25 g of a brown solid that was insoluble in common solvents.

The filtrate from the reaction was reduced to a total volume of 20 mL under vacuum and transferred via syringe onto a chromatography column packed with activated alumina (50 × 2 cm). Elution with CH_2Cl_2 gave an initial light green band containing Ni organometallics, including Cp_2Ni according to mass spectrometry. The second band (olive green) was collected and stripped of solvent under vacuum to leave dark green crystalline **10**. This solid was recrystallized from CH_2Cl_2/hexane for analysis: yield 0.10 g (15%); mp 300 °C. Anal. Calcd for $(Cp'Mo)_2(CpNi)_2S_4$ ($C_{22}H_{24}Mo_2Ni_2S_4$): C, 36.38; H, 3.33; S, 17.67. Found: C, 35.54; H, 3.22; S, 17.71.

Description of the Cyclic Voltammetry Experiment. Cyclic voltammetric studies were performed under nitrogen atmosphere in a three-compartment, three-electrode cell. One compartment contained a platinum-wire working electrode and a platinum-foil auxiliary electrode in close proximity to limit cell resistance. The reference compartment employed a silver-plated platinum wire. A buffer compartment between the working and reference compartments prevented cross-contamination of the cells. All three compartments were joined via fine glass frits to limit diffusion between them. A stock solution of 0.10 M Et_4NBF_4 in acetonitrile was used in all three compartments. The reference cell contained in addition 0.01 M $AgNO_3$, while the sample cell contained a 0.001 M solution of the cluster of interest (or less, depending on solubility).

Acetonitrile was purified by allowing it to stand over CaH_2 for several days, followed by distillation from CaH_2, fractional distillation from P_2O_5 (81–82 °C fraction was collected), and, finally, distillation again from CaH_2 just prior to use. Tetraethylammonium tetrafluoroborate was dried in vacuo (0.1 mmHg) at 110 °C for 6 h and stored under N_2 until used.

Platinum electrodes were cleaned by soaking them in acidic dichromate solution for 6 h and washing with water and acetone before drying. Sweeping of the electrodes between the potential limits of the solvent system completed the cleaning procedure.

A Princeton Applied Research Model 173 potentiostat equipped with a Model 176 current to voltage converter was used to control and monitor input/output to/from the electrodes. A Textronix FG 504 50-MHz waveform generator was used to supply the triangle wave. A Hewlett-Packard 7005B X-Y recorder was used for voltammogram recording.

A small crystal of ferrocene was added to the working cell at the end of an experiment and the ferrocene/ferrocenium redox wave recorded over the voltammogram in order to provide an internal reference that can be compared with other work.

(43) Seyferth, D.; Henderson, R. C.; Song, L. C. *Organometallics* **1982**, *1*, 125.
(44) Bogan, L. E.; Leach, D. A.; Rauchfuss, T. B. *J. Organomet. Chem.* **1983**, *250*, 429.
(45) Curtis, M. D.; Fotinos, N. A.; Messerle, L.; Sattelberger, A. P. *Inorg. Chem.* **1983**, *22*, 1559.

Table VII. Crystallographic Statistics

	$Cp'_2Mo_2Fe_2(CO)_8S_2$ (**3b**)	$Cp'_2Mo_2Co_2(CO)_4S_3$ (**6**)	$Cp'_2Mo_2Ni_2(CO)_2S_4$ (**9**)
color	brown	black	dark green
chem formula	$C_{20}H_{14}O_8Fe_2Mo_2S_2$	$C_{16}H_{14}O_4Co_2Mo_2S_3$	$C_{14}H_{14}O_2Mo_2Ni_2S_4$
mol wt	750.04	676.21	651.80
space group	$P\bar{1}$	$P\bar{1}$	$P2_1/n$
a, b, c, Å	9.219 (2), 6.899 (2), 10.441 (2)	10.404 (3), 11.015 (3), 9.962 (2)	9.712 (2), 20.303 (4), 9.787 (1)
α, β, γ, deg	73.34 (2), 113.68 (2), 95.98 (2)	99.78 (2), 96.99 (2), 63.11 (2)	98.30 (1)
V, Å^3	582.5 (3)	1002.0 (4)	1909.5 (6)
Z	1	2	4
ρ_{calcd}, g/cm^3	2.14	2.24	2.27
ρ_{obsd}, g/cm^3	2.12 (flotation)	2.30 (flotation)	2.24 (flotation)
cryst dimens, mm	0.221 × 0.184 × 0.191	0.080 × 0.140 × 0.480	0.278 × 0.159 × 0.297
μ(Mo Kα), cm^{-1}	24.66	31.42	36.35
scan speed, deg/min	2.5–12, variable	2.5–12, variable	2.5–12, variable
scan range	Mo Kα_1 − 0.8° to Mo Kα_2 + 0.8°	Mo Kα_1 − 0.8° to Mo Kα_2 + 0.8°	Mo Kα_1 − 0.8° to Mo Kα_2 + 1.0°
bkgd/scan time	0.8	0.8	0.8
2θ, deg	55	50	45
reflcns measd	$+h,\pm k,\pm l$	$+h,\pm k,\pm l$	$+h,+k,\pm l$
no. of reflcns	2850 (2357 with $I \geq 3\sigma(I)$)	3785 (2988 with $I \geq 3\sigma(I)$)	2955 (2179 with $I \geq 3\sigma(I)$)
N_o/N_v	15.3	12.2	10.0
goodness of fit	2.44	1.84	2.60
R_1, R_2	0.047, 0.063	0.036, 0.053	0.049, 0.066
residual, e/Å^3	1.59	0.72	0.88
largest shift/error on final cycle	2.62	0.07	0.42

Table VIII. Fractional Atomic Coordinates for $Cp'_2Mo_2Fe_2(CO)_8S_2$ (**3b**)

atom	x	y	z
Mo	0.8519 (0)	0.4613 (1)	0.8978 (0)
Fe	0.9201 (1)	0.3088 (1)	1.1928 (1)
S	0.9595 (1)	0.7827 (2)	0.9267 (1)
C1	0.6078 (7)	0.5416 (9)	0.6903 (6)
C2	0.7206 (7)	0.4850 (9)	0.6466 (6)
C3	0.7696 (7)	0.2811 (10)	0.7250 (7)
C4	0.6826 (7)	0.2066 (10)	0.8143 (7)
C5	0.5852 (6)	0.3679 (10)	0.7952 (7)
C6	0.5217 (8)	0.7430 (11)	0.6339 (8)
C7	0.7452 (6)	0.5435 (9)	1.0104 (6)
C8	1.0535 (8)	0.1439 (10)	1.3530 (7)
C9	0.7539 (8)	0.1419 (10)	1.1828 (8)
C10	0.8976 (8)	0.4818 (12)	1.2839 (7)
O7	0.6513 (5)	0.6345 (7)	1.0177 (5)
O8	1.1419 (7)	0.0345 (9)	1.4552 (6)
O9	0.6521 (6)	0.0307 (9)	1.1762 (8)
O10	0.8853 (8)	0.5890 (11)	1.3430 (7)

Table IX. Fractional Atomic Coordinates for $Cp'_2Mo_2Co_2(CO)_4S_3$ (**6**)

atom	x	y	z
Mo1	0.6408 (1)	0.2239 (1)	0.2978 (1)
Mo2	0.3826 (1)	0.2559 (1)	0.1936 (1)
Co1	0.4659 (1)	0.4505 (1)	0.1930 (1)
Co2	0.4633 (1)	0.2009 (1)	0.4483 (1)
S1	0.5630 (2)	0.2496 (2)	0.0671 (2)
S2	0.5601 (2)	0.0518 (2)	0.2700 (2)
S3	0.4205 (2)	0.4021 (2)	0.3863 (2)
O1	0.6567 (6)	0.5808 (6)	0.2116 (6)
O2	0.2091 (6)	0.6599 (6)	0.0719 (6)
O3	0.2053 (6)	0.2070 (6)	0.5435 (7)
O4	0.6522 (7)	0.1199 (6)	0.6903 (6)
C1	0.5808 (7)	0.5304 (7)	0.2074 (7)
C2	0.3093 (8)	0.5769 (7)	0.1186 (7)
C3	0.3083 (8)	0.2024 (7)	0.5038 (7)
C4	0.5765 (8)	0.1538 (7)	0.5964 (7)
C5	0.8623 (7)	0.2189 (8)	0.2667 (8)
C6	0.8092 (7)	0.3091 (8)	0.3889 (8)
C7	0.8016 (7)	0.2335 (8)	0.4839 (8)
C8	0.8500 (7)	0.0955 (8)	0.4221 (8)
C9	0.8902 (7)	0.0883 (8)	0.2887 (9)
C10	0.963 (1)	−0.043 (1)	0.190 (1)
C11	0.1705 (7)	0.3704 (8)	0.0607 (8)
C12	0.2454 (8)	0.2360 (9)	−0.0057 (8)
C13	0.2495 (8)	0.1446 (8)	0.0783 (9)
C14	0.1761 (8)	0.2229 (9)	0.1961 (9)
C15	0.1292 (7)	0.3623 (8)	0.1854 (8)
C16	0.038 (1)	0.484 (1)	0.289 (1)

Table X. Fractional Atomic Coordinates for $Cp'_2Mo_2Ni_2(CO)_2S_4$ (**9**)

atom	x	y	z
Mo1	0.3791 (1)	0.1615 (1)	0.8995 (1)
Mo2	0.3128 (1)	0.1188 (1)	0.6227 (1)
Ni1	0.5815 (1)	0.1386 (1)	0.7398 (1)
Ni2	0.3765 (1)	0.2468 (1)	0.6848 (1)
S1	0.5516 (3)	0.2309 (1)	0.8645 (3)
S2	0.4730 (3)	0.1809 (1)	0.5355 (3)
S3	0.1950 (2)	0.1968 (1)	0.7368 (3)
S4	0.4460 (2)	0.0637 (1)	0.8039 (2)
O1	0.868 (1)	0.103 (1)	0.753 (1)
O2	0.334 (1)	0.382 (1)	0.597 (1)
C1	0.756 (1)	0.116 (1)	0.748 (1)
C2	0.351 (1)	0.329 (1)	0.632 (1)
C3	0.403 (1)	0.106 (1)	1.113 (1)
C4	0.444 (1)	0.170 (1)	1.142 (1)
C5	0.330 (2)	0.210 (1)	1.106 (1)
C6	0.219 (1)	0.172 (1)	1.055 (1)
C7	0.259 (1)	0.106 (1)	1.059 (1)
C8	0.169 (2)	0.047 (1)	1.018 (1)
C9	0.280 (1)	0.044 (1)	0.434 (1)
C10	0.195 (1)	0.099 (1)	0.398 (1)
C11	0.096 (1)	0.101 (1)	0.486 (1)
C12	0.121 (1)	0.047 (1)	0.581 (1)
C13	0.236 (1)	0.011 (1)	0.545 (1)
C14	0.286 (1)	−0.053 (1)	0.603 (1)

X-ray Structure Determinations. 3b. Single crystals of **3b** were obtained by slow diffusion of hexane into a saturated CH_2Cl_2 solution at ambient temperature. X-ray data were collected[46] and the heavy atoms located with MULTAN.[47] Remaining atoms were located in subsequent difference maps, and all non-hydrogen atoms were refined to anisotropic convergence.[47,48] An absorption correction was not performed. Crystal

(46) A Syntex $P2_1$ four-circle diffractometer was employed for X-ray analysis. Crystal lattice parameters were typically determined from a least-squares refinement of 15 reflection settings obtained from the automatic centering routine. Intensity data were obtained at 22 °C with Mo K radiation (λ = 0.71069 Å) monochromatized by a graphite crystal. Three standard reflections were measured every 50 reflections.

(47) Computations were carried out on an Amdahl 470/V7 computer at The University of Michigan Computing Center. Programs used during the structure analysis were SYNCOR (data reduction by W. Shmonsees), MULTAN78 (direct methods by Peter Main), FORDAP (Fourier synthesis by A. Zalkin), ORFLS (full-matrix least-squares refinement by Busing, Martin, and Levy), ORFFE (distances and angles and their esd's by Busing, Martin, and Levy), and ORTEP (thermal ellipsoid plots by C. K. Johnson). ABSORB (absorption correction by D. Templeton and L. Templeton), HFINDR (calculation of hydrogen positions by A. Zalkin), and PLANES (calculation of least-squares planes by D. M. Blow) were used as specified in the text. The atom scattering factors were obtained from: *International Tables for X-ray Crystallography*; Kynoch: Birmingham, England, 1974; Vol. IV, Tables 2.2 and 2.3.1.

and data statistics are given in Table VII. Final positional and thermal parameters with estimated standard deviations are given in Tables VIII and XIS (S indicates supplementary material), respectively.

6. Single crystals of **6** were obtained by slow evaporation of a CH_2Cl_2/hexane solution at ambient temperature under N_2 atmosphere. X-ray data were collected[46] and the structure solved as described above. An absorption correction was not performed. Crystal and data statistics are given in Table VII. Final positional and thermal parameters with estimated standard deviations are given in Tables IX and XIIS, respectively.

9. Single crystals of **9** were obtained by slow cooling of a CH_2Cl_2/hexane solution to −5 °C. X-ray data were collected[46] and solved for heavy atoms with MULTAN.[47] Remaining atoms were located in subsequent difference maps, and all non-hydrogen atoms were refined to anisotropic convergence.[47,48] Hydrogen atom positions were calculated but were kept fixed during the final cycles of refinement. An absorption correction was not employed. Crystal and data statistics are given in Table VII. Final positional and thermal parameters with estimated standard deviations are given in Tables X and XIIIS, respectively.

4a. Single crystals of **4a** were obtained by slow diffusion of hexane into a saturated CH_2Cl_2 solution at ambient temperature. Our unit cell constants and spectroscopic data were in good agreement with those reported.[23a]

4w. Single crystals of **4w** were obtained by slow diffusion of hexane into a saturated toluene solution at ambient temperature. Determination of unit cell parameters (a = 18.00, b = 8.35, c = 16.03 Å; β = 114.3°) indicated that the crystals were isomorphous with the analogous Mo butterfly cluster **4a**.

7. Single crystals of **7** were obtained by slow diffusion of hexane into a saturated CH_2Cl_2 solution at ambient temperature. Our unit cell parameters and spectroscopic data were in good agreement with those reported.[27]

Acknowledgment. This work was supported in part by the National Science Foundation (Grant No. CHE-8305235). P.D.W. is grateful to the donors of the Samuel H. Baer and Rackham Predoctoral Fellowships. We also thank Professors P. Braunstein and M. Rakowski DuBois for sharing their results prior to publication.

Supplementary Material Available: For **3b**, **6**, and **9**, Tables XIS–XIIIS, listing thermal parameters (B_{ij}), and, for **3b**, Figures 6 and 7, showing cyclic voltammograms (5 pages); for **3b**, **6**, and **9**, Tables XIV–XVIS, listing F_o and F_c (31 pages). Ordering information is given on any current masthead page.

(48) Refinement entailed minimizing the function $\sum w(|F_o| - |F_c|)^2$, where $|F_o|$ and $|F_c|$ were the observed and calculated structure factor amplitudes. The weighting factors w were taken as $w = 4F_o^2/(\sigma^2(F_o^2) + (PF_o^2)^2)$, where P, the factor preventing overweighting of strong reflections, was set equal to 0.04. The agreement indices $R_1 = \sum||F_o| - |F_c||/\sum|F_o|$ and $R_2 = (\sum w(|F_o| - |F_c|)^2\sum wF_o^2)^{1/2}$ were used to evaluate the refinement.
(49) Alper, H.; Einstein, F. W. B.; Harstock, F. W.; Willis, A. C. *J. Am. Chem. Soc.* **1985**, *107*, 173.
(50) Stevenson, D. L.; Dahl, L. F. *J. Am. Chem. Soc.* **1967**, *89*, 3721.
(51) Vergamini, P. J.; Vahrenkamp, H.; Dahl, L. F. *J. Am. Chem. Soc.* **1971**, *93*, 6327.
(52) Bandy, J. A.; Davies, C. E.; Green, J. C.; Green, M. L. H.; Prout, K.; Rodgers, D. P. S. *J. Chem. Soc., Chem. Commun.* **1983**, 1395.
(53) McKenna, M.; Wright, L. L.; Miller, D. J.; Tanner, L.; Haltiwanger, R. C.; Rakowski DuBois, M. *J. Am. Chem. Soc.* **1983**, *105*, 5329.
(54) Casewit, C. J.; Haltiwanger, R. C.; Noordik, J.; Rakowski DuBois, M. *Organometallics* **1985**, *4*, 119.
(55) Rakowski DuBois, M.; VanDerveer, M. C.; DuBois, D. L.; Haltiwanger, R. C.; Miller, W. K. *J. Am. Chem. Soc.* **1980**, *102*, 7456.
(56) Silverthorn, W. E.; Couldwell, C.; Prout, K. *J. Chem. Soc., Chem. Commun.* **1978**, 1009.
(57) Connelly, N. G.; Dahl, L. F. *J. Am. Chem. Soc.* **1970**, *92*, 7470.

Contribution from the Department of Chemistry,
North Carolina State University, Raleigh, North Carolina 27695-8204

Syntheses and Characterization of Two Vanadium Tris Complexes of the 1,2-Dithiolene 5,6-Dihydro-1,4-dithiin-2,3-dithiolate. Crystal Structure of $[(C_4H_9)_4N][V(DDDT)_3]$[1]

Jane Hanna Welch, Robert D. Bereman,* and Phirtu Singh

Received December 9, 1987

The reaction between VCl_3 and the dipotassium salt of the new dithiolene 5,6-dihydro-1,4-dithiin-2,3-dithiolate, $DDDT^{2-}$, resulted in the isolation of $V(DDDT)_3^-$ as the tetraalkylammonium salt. This reaction, under oxygen-free conditions, yields the dianion, $V(DDDT)_3^{2-}$, also isolated as the tetraalkylammonium salt. A single-crystal structural study of the tetrabutylammonium salt of $V(DDDT)_3^-$ has been performed and is the first reported crystal structure of a monoanionic vanadium dithiolene. The salt crystallizes in the orthorhombic space group $P2_12_12_1$ with a = 10.425 (4) Å, b = 19.596 (9) Å, and c = 38.53 (2) Å. The large unit cell contains eight cations and eight anions with two complete molecules in the asymmetric unit. In each of the unique anions, the six ligated sulfur atoms form a slightly distorted trigonal prism about the vanadium with average V–S distances of 2.338 (4) and 2.343 (4) Å, respectively. Two parameters relevant to trigonal-prismatic coordination are an average S–V–S (trans) angle of 135.5 (2)° and an average twist angle of 3.7°. While the formal oxidation states of $V(DDDT)_3^-$ and $V(DDDT)_3^{2-}$ are V and IV, respectively, evidence presented here indicates that the monoanion is more correctly formulated as a V(III) complex with the ligands being intermediate between dithiodiketone and dithiolate.

Introduction

The coordination chemistry of transition-metal dithiolenes has been an area of great interest for a number of years. Yet, the first analytically pure tris(dithiolene), $Mo[S_2C_2(CF_3)_2]_3$, was prepared by King[2] in 1963. This class of compounds yielded the highly unusual trigonal-prismatic (TP) geometry in the structures of $Mo(S_2C_2H_2)_3$, $Re(S_2C_2Ph_2)_3$, and $V(S_2C_2Ph_2)_3$.[3-5] It is known that tris complexes like their bis counterparts undergo reversible one-electron-transfer reactions resulting in stable species differing in oxidation state. These observations brought about a flurry of research on tris(dithiolenes).[6-10]

Since the initial report of the synthesis of the new dithiolene potassium 5,6-dihydro-1,4-dithiin-2,3-dithiolate[11] (K_2DDDT) shown in Figure 1, only the chemistry with the latter transition metals Ni, Pd, Pt, Cu, and Au has been investigated.[12,13] In our efforts to more fully understand the coordination chemistry of the

* To whom correspondence should be addressed.

(1) Coordination Chemistry of New Sulfur Containing Ligands. 28.
(2) King, R. B. *Inorg. Chem.* **1963**, *2*, 641.
(3) Smith, A. E.; Schrauzer, G. N.; Mayweg, V. P.; Heinrich, W. *J. Am. Chem. Soc.* **1965**, *87*, 5798.
(4) Eisenberg, R.; Ibers, J. A. *Inorg. Chem.* **1966**, *5*, 411.
(5) Eisenberg, R.; Gray, H. B. *Inorg. Chem.* **1967**, *6*, 1844.
(6) McCleverty, J. A. *Prog. Inorg. Chem.* **1968**, *10*, 49 and references therein.
(7) Schrauzer, G. N. *Transition Met. Chem. (N.Y.)* **1968**, *4*, 299.
(8) Eisenberg, R. *Prog. Inorg. Chem.* **1970**, *12*, 295.
(9) Burns, R. P.; McAuliffe, C. A. *Adv. Inorg. Chem. Radiochem.* **1979**, *22*, 303.
(10) Mahadevan, C. *J. Crystallogr. Spectrosc. Res.* **1986**, *16*, 347.
(11) Vance, C. T.; Bereman, R. D.; Bordner, J.; Hatfield, W. E.; Helms, J. H. *Inorg. Chem.* **1985**, *24*, 2905.
(12) Vance, C. T. Ph.D. Thesis, North Carolina State University, 1985; p 44.

0020-1669/88/1327-2862$01.50/0